ANALYSIS OF ELECTROMAGNETIC DEVICES USING THE PRINCIPLE OF DUALITY BETWEEN ELECTRICAL AND MAGNETIC CIRCUITS TOGETHER WITH FINITE ELEMENT ANALYSIS

Antônio Flavio Licarião Nogueira[1] & Leonardo Jose Amador Salas Maldonado[2]
[1,2]Universidade do Estado de Santa Catarina, Joinville, Santa Catarina, Brazil

ABSTRACT

Based on the limitations of classical magnetic circuit analysis, the paper addresses the use, in conjunction, of finite element analysis and the principle of duality of interlinked electrical and magnetic circuits. The device used in the derivation of equivalent electric circuits and finite-element models is an industrial alternating current (*AC*) contactor rated for 220 volts, 60 hertz. Two operating conditions are considered: a locked closing maneuver and the closed-core configuration. It is presented a step-by-step procedure to obtain an averaged value for the relative permeability used in the calculation of the reluctors that form magnetic circuits. For the two operating conditions, the contactor's magnetizing inductances are obtained from electrical dual circuits and compared with values obtained from time-harmonic finite element simulations. Finally, it is presented a detailed analysis of the distribution of magnetic energy storage in different regions of the device's numerical model.

Keywords: *Contactor, Duality model, Energy storage, Finite element analysis, Magnetic circuits, Magnetic forces.*

1. INTRODUCTION

The techniques used in the analysis of electromagnetic devices may be divided into two classes: the traditional techniques and the numerical techniques. The traditional techniques are based on magnetic circuit analysis and make use of relatively simple equations like magnetic Ohm's law. The more recent, computer-based techniques have been developed for solving the magnetic field equations numerically, and are capable of manipulating large volumes of data at very high speeds. The principal advantage of the numerical approaches is the ability to easily accommodate new inspections, new device's configurations. Analysis techniques based uniquely on magnetic circuit analysis have the disadvantage of generating quantitative results that are not very reliable. On the other hand, these results are fast to obtain, easy to interpret, and the analysis task usually brings insight into the subject. It is possible, however, to treat the traditional and numerical techniques as complementary design tools. One example of these complementary approaches is the use of the classical Biot-Savart law together with the numerically implemented method of impedances to solve the forward problem in magnetic induction tomography systems [1]. Another successful combination of traditional and modern techniques is the use of finite-element based programs to generate the data required in the analysis tasks of power transformers based on the method due to E.C. Cherry and known as duality principle [2]. The duality approach is an essential tool for the analysis of complicated magnetic structures such as multiwinding power transformers. Electrical dual circuits have been extensively applied in conjunction with computer programs known as Electromagnetic Transients Program (EMTP)-type in the analysis of leakage inductances of multisection power transformers [3]. Electrical duals have also been applied in the development of advanced numerical models that represent the magnetic core of multiwinding power transformers [4].

The purpose of this paper to show how the principle of duality between interlinked electric and magnetic circuits can be used in conjunction with finite element simulations. The device used in the derivation of equivalent electric circuits and finite-element models is an industrial alternating current (*AC*) contactor rated for 220 volts, 60 hertz. A detailed study of this contactor using time-harmonic finite element simulations supported by conventional electric circuits and measurements is presented in [5]. A photograph showing details of the contactor's electromagnet *double-E* core at closed position, the location of air-gap regions and shading coils appears in figure 1(a). The photograph presented in figure 1(b) exhibits details of the fixed-core laminations, the right-hand side shading coil, as well as a search coil placed on the left-hand side pole and used to measure eddy currents.

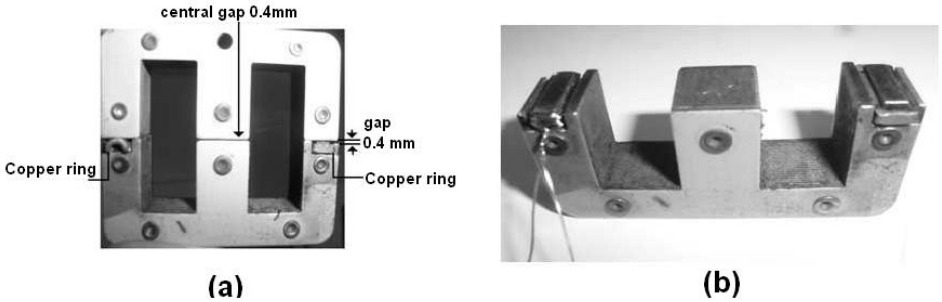

Figure 1. (a) The magnetic core at closed position; (b) Details of the fixed-core laminations.

2. PROBLEM DESCRIPTION

The contactor's electromagnet is the component that directly affects its electromagnetic action. The electromagnet of this particular contactor consists of a 5,000-turn coil wound around the central limb of the lower or stationary portion of the *double-E* laminated core. For the closed-core configuration, the size of each rectangular window is 3.2 cm by 1.05 cm. The height of the driving coil is approximately 1.4 cm. The main geometrical dimensions are indicated in figure 2, and the depth of the device is 1.2 cm.

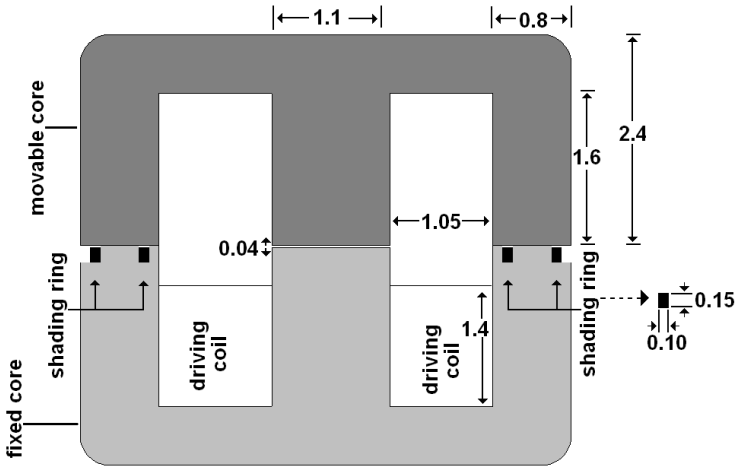

Figure 2. Sketch of the contactor's electromagnet, dimensions in centimeter. Not to scale.

The contact between the two magnetized portions of the *E*-shaped magnetic cores is, in fact, restricted to small regions located at the side limbs. The innermost portions of the magnetized surfaces in contact are known as unshaded poles, whereas the regions surrounded by the shading rings are known as shaded poles. These geometrical features are illustrated in figure 3(a). The gap separating the two portions of the central limb is 8.0 mm when the contactor is open and only 0.4 mm at the closed core configuration.

The symmetry of the winding and *E*-shaped magnetic cores with respect to the line of symmetry *YY'* indicated in figure 3(a) allows the creation of the simplified magnetic structure that appears in figure 3(b), wherein the outer limbs are combined into equivalent limbs with twice the area transverse to the circulating magnetic flux or magnetic section. In this way, the structure is divided into regions of similar magnetic section. As a result, both the number of flux paths and the number of circuit elements are reduced. The simplified magnetic structure will be used in the creation of the dual equivalent electrical circuit as well as in the finite element simulations. In the illustrations of figure 3, w_c denotes the width of the central limb, and w the width of the outer limbs.

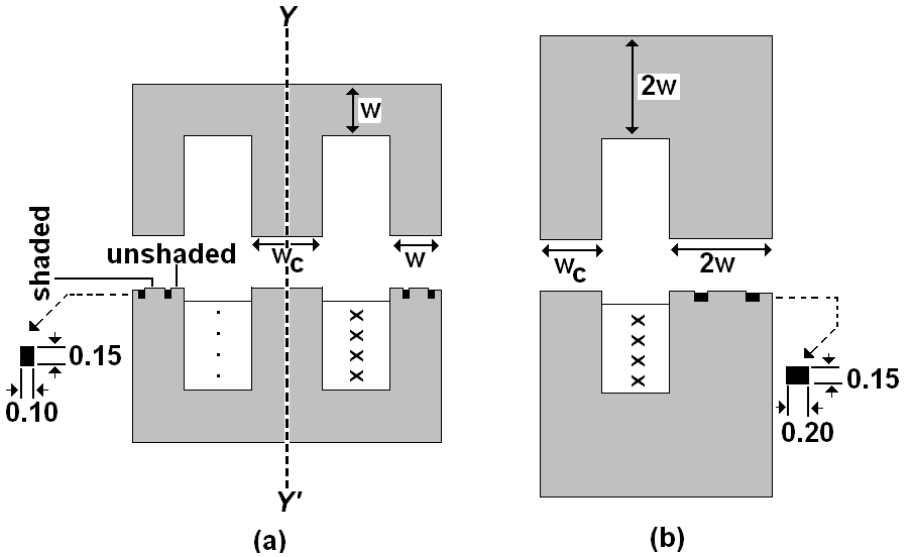

Figure 3. (a) Cross-sectional view of the contactor; (b) Simplified magnetic structure.

2.1. Operating conditions

AC contactors may be described by the conventional electric circuit shown in figure 4. The components of the circuit correspond to the physical phenomena in the device. The resistor R_w in the horizontal branch accounts for the ohmic loss in the winding of the exciting coil. The magnetizing inductance is represented by the inductor *L* in the vertical branch, and accounts for the magnetic field energy storage in the magnetic cores and leakage fields in the windows and air gaps. The shunt resistor *R* in the vertical branch represents the active power loss in the magnetic cores.

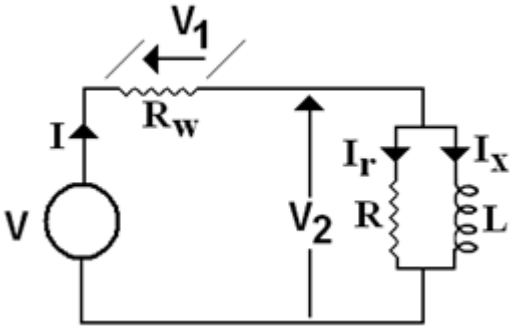

Figure 4: Conventional equivalent electric circuit of the contactor.

Depending on the operating condition, the value of the elements that form the parallel *RL* impedance may change substantially, and this affects the magnitude and phase of the driving current *I*. In this study, two operating conditions are analyzed. The first one represents a locked closing maneuver, whereas the second one refers to the contactor's "making" operation, i.e., the condition where the driving coil is excited by rated current and the movable and fixed cores are in contact. From now on, this operating condition will be referred to as the closed core configuration. To enable the measurement of the terminal electric quantities related to the locked closing maneuver, the armature movement has been blocked by the presence of a non-magnetic rubber spacer 8 millimeter high inserted in the air-gap regions that separate the fixed and movable cores.

2.2. The current-driven finite element software *FEMM*

The two-dimensional simulation software *FEMM* has been used to obtain the 60 Hz time-harmonic finite-element solutions [6]. This is a current-driven finite-element program that works with prescribed currents rather than voltages. In the suite of programs *FEMM*, *AC* driving currents must be specified by means of peak values.

Measurements of the terminal currents have been carried out by applying sinusoidal voltages close to 220 V to the end terminals of the 5,000-turn contactor driving coil. During the measurements, it has been observed that currents are nonsinusoidal, especially at the closed operation. To overcome this difficulty, the current waveforms have been registered and values of the "true" root-mean-square (*rms*) have been computed by numerical integration. Peak

values of currents have then been computed employing the "true rms" approximations. Data related to the "true" *rms* computed currents, together with calculated peak values are resumed in table 1.

Table 1. Contactor's terminal voltages and currents.

Configuration	**Applied *rms* voltage (V)**	**Current (mA)**	
		true root-mean square	**peak**
Locked closing maneuver	218.00	268.00	379.01
Closed core	222.00	50.50	71.42

3. MAGNETIC CIRCUIT ANALYSIS

Magnetic circuit analysis is based on magnetic circuits that contain sources of magnetomotive forces and a number of interconnected lumped elements known as reluctors. These components represent the storage of magnetic energy in magnetic cores, air gaps, fringing flux around the gaps, and leakage fields. In the definition of the lumped elements, each region where the magnetic flux density ***B*** is more or less uniform is represented by an element of a given magnetic reluctance. Magnetic Ohm's law states the relationship between the variables,

$$F = \Re\phi, \tag{1}$$

where F is the magnetomotive force, $\Re$ is the magnetic reluctance, and ϕ is the magnetic flux.

In order to derive the magnetic circuit, the reluctance of each separate region of the magnetic structure is calculated from its area A, length l and magnetic permeability by

$$\Re = \frac{l}{\mu_r \mu_0 A}, \tag{2}$$

where μ_r is the region's relative permeability, and $\mu_0 = 4\pi \times 10^{-7}$ H/m is the permeability of free space.

3.1. Limitations of magnetic circuit analysis

Calculation of magnetic reluctance is not a trivial task, as it may suggest at a first glance. Difficulties arising from three different sources are discussed in the following. In order to take into account the fringing flux around the gaps that separate two magnetized sections of a device, it is necessary to increase the gap area transverse to the circulating flux. The enlarged gap area is usually referred to as effective gap area, and may be calculated by empirical formulae. One way of calculating the enlarged area consists in multiplying the original gap area by a fringing correction factor F given by

$$F = 1 + \frac{l_g}{S^{1/2}} \ln\left(\frac{2G}{l_g}\right), \tag{3}$$

where l_g is the gap length, S is the cross-section of the poles, and G is the winding length of the driving coil present in contactors and gapped inductors [7]. A very popular correction method consists in adding the length of the gap to the dimensions (width and depth) of each pole cross section. The latter approach is not problem-dependent and will be used in the calculations of effective gap areas presented in a later section.

The calculation of the stray field outside the core of contactors and inductors, for example, is very important but extremely difficult to perform analytically. The definition of the mean path length l of the stray field is usually a guess, a choice based on trial-and-error, and requires a deep understanding of the device's physical behavior, as well as familiarity with the expected solution.

3.2. Complexity of magnetic material representation

The main difficulty in calculating magnetic reluctances is actually related to the analytical and/or numerical modelling of the magnetic material properties. The magnetic permeability, for example, is computed from the slope of *B*-*H* curves by

$$\mu = \frac{\partial B}{\partial H}, \tag{4}$$

and the range of slopes, known as incremental permeabilities, is usually very wide. Even when dealing with continuous and smooth mean magnetization curves (or *B*-*H* curves), the slopes encountered in the magnetically linear region are usually much larger than the ones found in the saturated region. In simpler magnetic circuit analysis, hand calculations using only two different relative permeabilities appear very frequently. In these calculations, one of the relative permeabilities is used to represent the whole range of linear or unsaturated

operation, and the other represents the range of saturated operation. In fact, the relative permeability of most magnetization characteristics varies in a continuous fashion as the driving current and the *H*-field increase, and the use of low-order piecewise linearized *B-H* characteristics may lead to inaccurate results.

The numerical modelling of magnetic material property curves is a notoriously difficult task [8], [9]. However, most electromagnetic field simulators contain "libraries" of material property curves for many soft and hard magnetic materials. The material properties always include the mean magnetization curve (or *B-H* curve) and, sometimes, additional curves related to loss at 50 and 60 Hz, and magnetostriction coefficient. The primary source of information to edit *B-H* curves is the materials manufacturer's catalogue. Data can also be obtained experimentally, from a series of concentric hysteresis loops. In this case, a preliminary, crude approximated curve is obtained by connecting the origin of the *B-H* plane and the vertices of the hysteretic loops. The photograph presented in figure 5 shows the contactor's core hysteresis loop for an applied *rms* voltage of 250 V. The device is rated for 220 V, but the contactor's coil is already submitted to an overvoltage of 13.6%. The vertices of this hysteresis loop would produce operating *B-H* points close to the "knee" of the curve but far away from the saturated region. Attempts to obtain wider loops and hence additional *B-H* points imply increased applied voltages and currents, and this may damage the device.

.

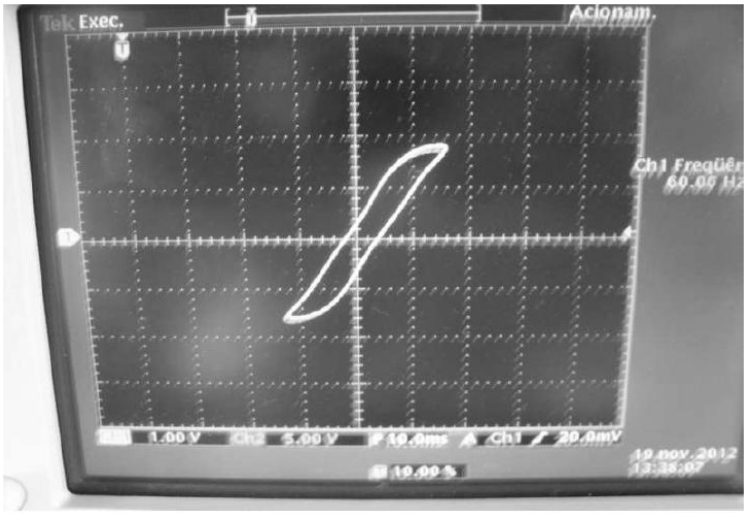

Figure 5. Hysteresis loop of the contactor's bulk lamination for an applied overvoltage of 13.6%.

Fortunately, modern field simulators use to extrapolate linearly off the end of the *B-H* curves edited by the user whenever the solver encounters operating *B-H* point levels that are out of the range of the input data. The use of a magnetization characteristic present in the field-simulator materials library that closely matches the low-level measured *B-H* points is sometimes a good practice. In this study, the latter approach to the choice of the *B-H* curve has been adopted. The homogeneous composite material, commercially known as "Carpenter Silicon Core Iron A, 1066C Anneal" is thus used to model all regions containing the thin laminations that form the contactor's magnetic cores. The *B-H* curve for this composite material is presented in figure 6. The curve presented in figure 7 represents the variation of this composite's relative permeability as function of the *H*-field.

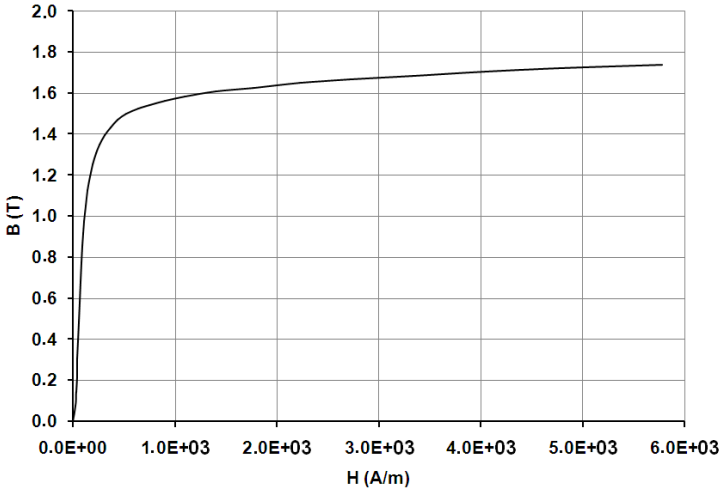

Figure 6. B-H curve for the composite material commercially known as "Carpenter Silicon Core Iron A, 1066C Anneal".

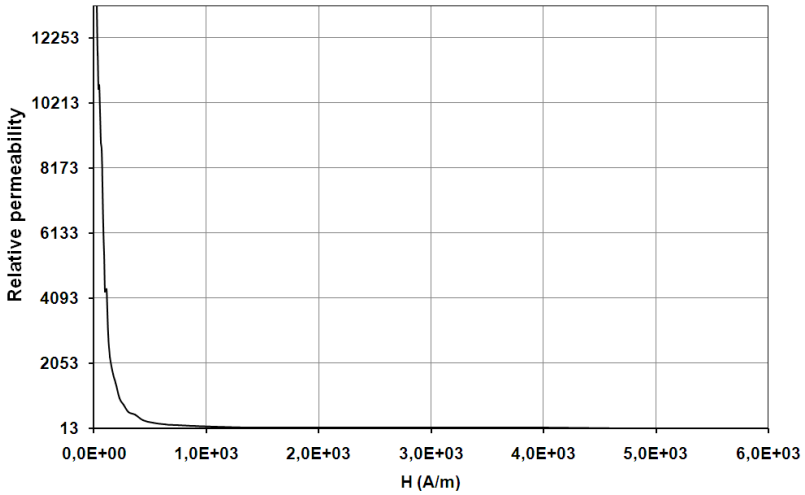

Figure 7. Variation of relative permeability as a function of the H-field for the "Carpenter Silicon Core Iron A, 1066C Anneal" composite.

A close observation of the characteristic presented in figure 7 helps to understand the difficulties related to the choice of the relative permeability μ_r assigned to a given region. It is usually very difficult to guess the relative permeability values that correspond, for example, to a set of measured flux densities *B*. With the aid of this characteristic, it is possible to observe a large variation of relative permeability values with respect to the increase of the *H*-field. In this particular plot, values of the relative permeability undergo a fold reduction of approximately 1,000 times along the excursion. The maximum value is equal to 13,239, the minimum value is equal to 13.45, and the mean value is 3,485.

4. ELECTRICAL DUALS AND FINITE ELEMENT ANALYSIS

One of the practical recommendations in the derivation of dual electrical circuits is related to the simplicity of the final electrical dual. The exploitation of the magnetic device's symmetry allied to the combination of magnetized sections with similar cross-sectional areas, for example, will certainly reduce the complexity of both, the magnetic structure and the related electric dual. A very important step in the derivation of electric duals is the definition of "reluctors", the lumped elements that represent the storage of magnetic energy. It is possible, at this stage, to make use of the high accuracy of finite element analysis and, for each magnetized portion of the device, assign a value of relative permeability (and reluctance) based on numerical field solutions. It is important to notice that, across most paths of magnetized cores, values of the relative permeability do vary, as illustrated in the following.

Consider a magnetic structure similar to the one shown in figure 3(b) and used to analyze the contactor's "making" operating condition. The gap separating the two portions of the central limb is only 0.4 mm. The movable core is in contact with both, the shaded and unshaded poles. The variation of the relative permeability along the mean path of

the equivalent outer limbs is exhibited in the graph of figure 8. Along this path, the magnetic section is twice that of the original structure shown in figure 3(a). In the graph of figure 8, the dash characteristic represents the variation of the relative permeability, and the permeability values have been obtained from the 60 Hz time-harmonic finite element solution. The solid line represents the averaged relative permeability.

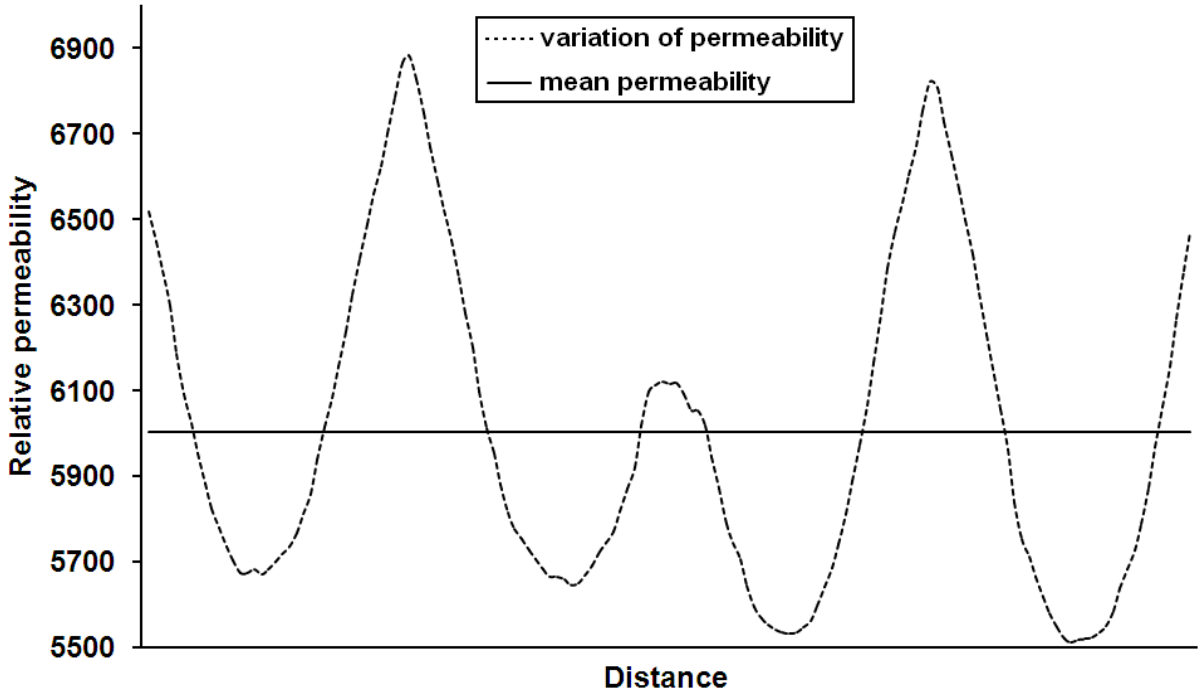

Figure 8. Averaged value and variation of the relative permeability along the outer limbs of the simplified magnetic structure.

Observation of this graph provides knowledge about what actually happens "inside" the magnetic structure: a continuous change in permeability values, from point to point. It is possible, however, to average the finite-element based relative permeability values, and use the mean value in the calculation of the reluctance of a given region. The approach of mean relative permeability to represent the relative permeability (and reluctance) of a given magnetized region has been chosen and will be applied in the derivation of electrical dual circuits for the *AC* contactor. The step-by-step procedure to obtain the mean relative permeability is presented in the following.

1. Get the field solution;
2. Define the contour that represents the mean path of the magnetic flux;
3. Choose the number of sampling points;
3. Get the line plot of the *H*-field magnitude and write data to a text file;
4. Get the line plot of the *B*-field magnitude and write data to a text file;
5. For each pair of successive *B*-*H* points, compute the relative permeability by

$$\mu_r = \frac{1}{\mu_0}\frac{\Delta B}{\Delta H}. \qquad (5)$$

6. Compute the mean relative permeability.

5. DERIVATION OF DUAL ELECTRICAL CIRCUITS

In order to derive the equivalent electrical circuit of a given device employing the duality between interlinked electric and magnetic circuits, the starting point may be a draft of a magnetic structure containing the parts that directly affect the electromagnetic action of the device under analysis [10]. The starting point of the present development is thus the simplified magnetic structure that appears in figure 3(b).

5.1. Contactor's locked closing maneuver

The required information to compute the reluctances of the eight regions that represent the contactor's open configuration are indicated in the illustration of figure 9(a). Geometrical data include the magnetic section of the

central limb S_c=1.32 cm^2, and the magnetic section of the equivalent outer limbs S_o=1.92 cm^2. The mean path length of the magnetic flux ϕ along each region is indicated separately in figure 9(b).

To reduce the number of elements of the magnetic circuit, the process can be further simplified by combining regions with same magnetic section. In this way, the two halves of the central limb are combined into a single reluctor with averaged relative permeability μ_{rc}=2616. Likewise, core regions above and below the gap are combined into a single reluctor with averaged relative permeability μ_{ro}=1858.

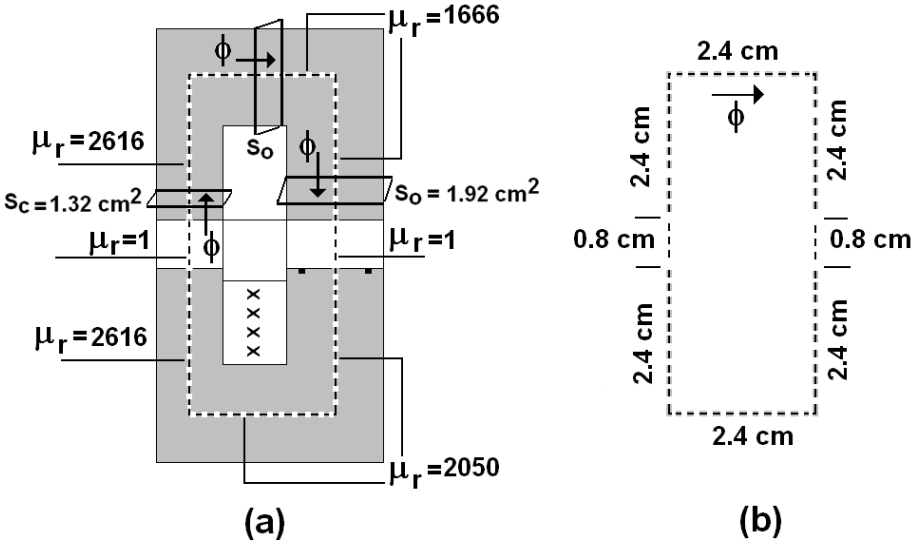

Figure 9: (a) Cross-sectional view of the simplified magnetic structure, and computed relative permeabilities;(b) Mean flux path lengths;

In the structure shown in figure 9(a), fringing flux around the air gaps is taken into account in the calculation by increasing the effective gap areas, i.e., by adding the length l_g of the gap to the dimensions (width and depth) of each core pole cross section. The resulting magnetic circuit is shown in figure 10(a). From now on, the subscripts "c" and "o" used to identify circuits' elements refer to the central limb and outer equivalent limb, respectively. Subscripts "cg" and "og" refer to the central gap and outer gap, respectively.

All dash lines that appear in the magnetic circuit of figure 10(b) connect nodes *x* and *y*, and cross all intervening elements of the magnetic circuit. In the creation of the dual electrical circuit, dash lines represent the branches of the equivalent electrical circuit, and the intervening elements become the transformed elements. The main magnetic-electrical duality relationships are summarized in table 2.

Table 2: Magnetic-electrical duality relationships.

Magnetic	**Electrical**
Nodes	Meshes
Open circuit	Short circuit
Series element	Parallel element
Magnetomotive force	Ampere-turns
Flux time variation (dϕ/dt)	Volts per turn
Reluctance	Permeance

The magnetic circuit shown in figure 10(b) should now be transformed into an equivalent electrical circuit wherein all values pertain to one-turn windings, and this may be referred to as the intermediate equivalent dual circuit. If *V* and *I* represent the terminal voltage and current of the *N*-turns winding or exciting coil in the actual magnetic device, *V/N* represents the terminal voltage and *NI* the terminal current of the intermediate equivalent dual circuit, respectively. The magnetic energy storage associated to each separate region of the magnetic structure is represented in the intermediate dual circuit by the region's permeance *P*, defined as the reciprocal of the magnetic reluctance and computed by

$$\mathrm{P} = \frac{1}{\Re} = \frac{\mu_r \mu_0 A}{l}. \qquad (6)$$

It is worth noting that each permeance *P* represents the inductance of an idealized winding with exactly one turn. In order to obtain the final equivalent dual circuit, all quantities of the intermediate circuit must be scaled, either up or down, to bring them into accord with the actual values. For a winding with *N* turns, the voltage per turn *V/N* is multiplied by *N* to become the terminal voltage *V*, and the ampere-turn *NI* is divided by N to become the terminal current *I*. In the same way, all permeance values should be multiplied by the number of turns squared N^2 to yield the actual inductance values. The intermediate or permeance model of the *AC* contactor is shown in the illustration of figure 11(a). The final electrical equivalent dual circuit with inductance values in henry is shown in figure 11(b). This circuit contains four inductive elements which represent the four reluctors in the original magnetic circuit. The four inductors combine to form a single equivalent inductor L_{eq}=0.82 henry, as shown in figure 11(c).

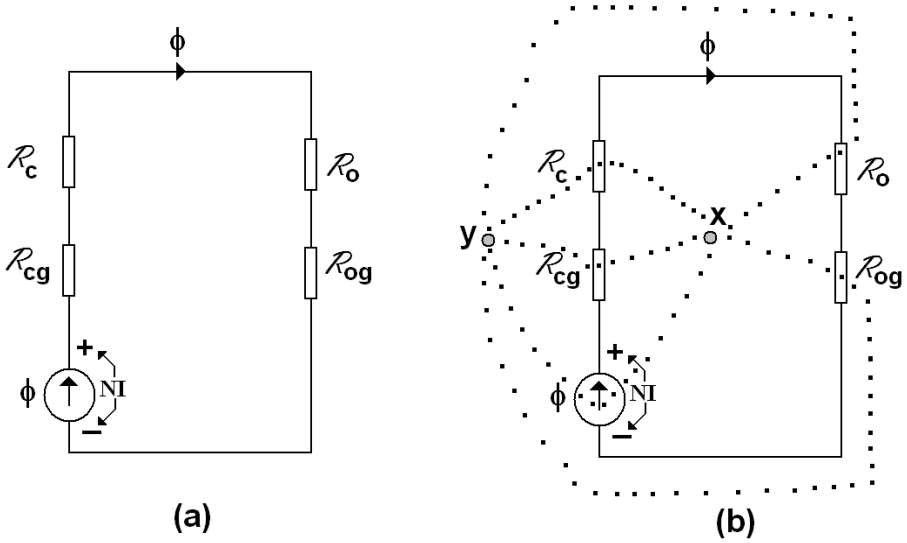

Figure 10. (a) Reluctance model for the contactor's open configuration; (b) Creation of the magnetic-electrical dual circuit.

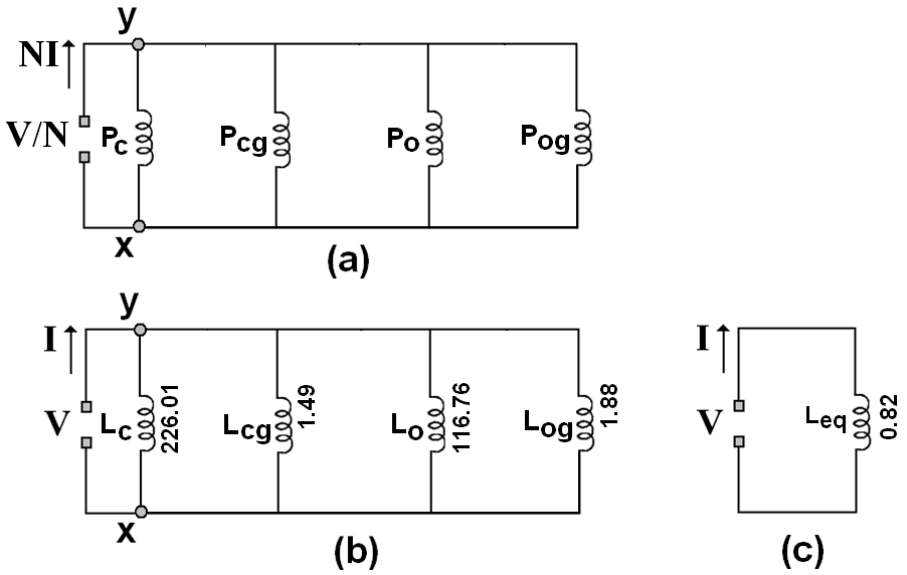

Figure 11. (a) Intermediate electrical dual circuit or permeance model; (b) Final electrical dual circuit; values of inductors in henry; (c) Final electrical dual circuit with the equivalent inductor.

5.2. Contactor's closed core configuration

The process of obtaining the electrical dual circuit that represents the contactor's closed core configuration is even simpler because the original magnetic structure and the equivalent electrical circuits contain fewer elements. When there is contact of the magnetic cores, the reluctance model contains only three reluctors representing the central gap and two core regions with same magnetic section. The first reluctor represents the two halves of the central limb with magnetic section of 1.32 cm^2 and averaged relative permeability μ_{rc}=3988. The second reluctor represents the

central gap. The third reluctor represents the combined outer limbs with magnetic section of 1.92 cm^2 and averaged relative permeability μ_{ro}=6001. The final electrical dual circuit for the closed core configuration with inductance values in henry is shown in figure 12(a). The circuit contains three inductive elements that combine to form a single equivalent inductor L_{eq}=10.46 henries, as shown in figure 12(b).

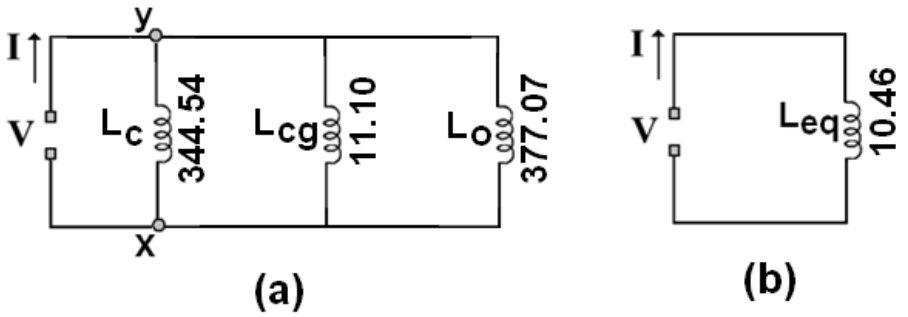

Figure 12. (a) Electrical dual circuit for the contactor's closed core configuration; (b) Dual circuit with the equivalent inductor.

6. NUMERICAL RESULTS

6.1. Magnetizing inductances

For the two operating conditions, the magnetizing inductances of the contactor have been determined using the dual electrical circuits and finite element simulations. Computed values are summarized in table 3. Per cent errors indicated in the table are computed taking the more precise finite-element estimates as benchmarks.

Table 3. Contactor's magnetizing inductances obtained by two different methods. Values in henry.

Configuration	**Dual electrical circuit**		**Finite elements**
	Inductance (H)	**Error**	**Inductance (H)**
Locked closing maneuver	0.82	26.1%	1.11
Closed core	10.46	4.4%	10.02

6.2. Magnetic energy storage

The analysis of magnetic energy storage in electromagnetic devices is a very important design task. This task is enormously facilitated by finite element simulations, mainly because the energies stored in different regions of a numerical model are separately computable. The total stored energy related to the locked closing maneuver amounts to 31.41 millijoules, approximately three times the stored energy of 11.09 millijoules related to the closed core configuration. Per cent values of the energy stored in different regions of the contactor is presented in the graph of figure 13. For each of the two operating conditions, percentages of the energy stored in the magnetic core and central gap are indicated separately. In the graph, the percentages indicated as "other regions" concern the energy stored in the coil, window, shading rings and air-filled regions surrounding the cores.

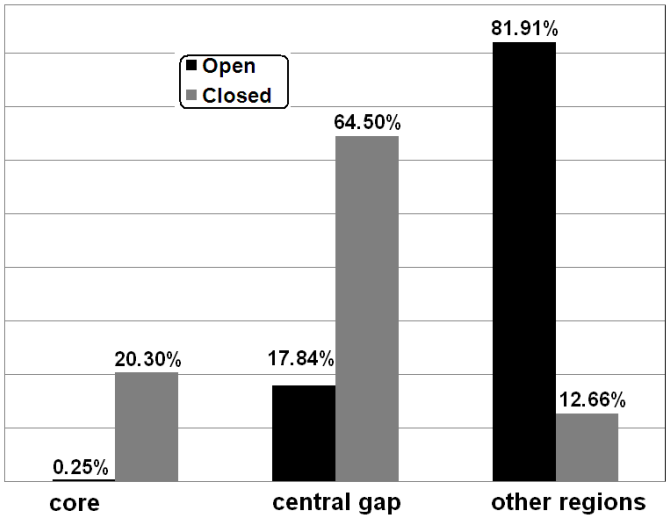

Figure 13. Per cent values of stored energy in different regions of the contactor's numerical model.

A close observation of the simulated data shows that, for the locked closing maneuver, less than 1.0% of the total energy is stored in the magnetic core. For this operating condition, the length of the central gap is 8.0 mm, and almost all the energy is stored in non-magnetic regions.

For the closed core configuration, 20.30% of the total energy is stored in the magnetic core. For this operating condition, the length of the central gap is only 0.4 mm, and this region stores 64.50% of the total energy. The inclusion of a tiny gap in the central limb may add manufacturing complications, but has the important effect of reducing the harmonic content of the magnetizing current.

7. CONCLUSIONS

The discussion places emphasis to the limitations of traditional magnetic circuit analysis, and proposes the combined use of traditional and modern techniques. Specifically, the discussion shows how to combine dual electrical circuits and finite element simulations in the analysis and characterization of an industrial *AC* contactor rated for 220 volts, 60 hertz. Two operating conditions are considered: a locked closing maneuver and the contactor's making operation. The main contributions of the work are related to: (i) the correct specification of alternating nonsinusoidal currents in current-driven finite-element programs; (ii) the detailed examination of the numerical operations necessary to obtain a unique averaged value of the relative permeability to be used in the calculation of reluctors; (iii) the quantitative analysis of the proportions of magnetic energy stored in the different regions of the device's numerical model.

8. ACKNOWLEDGEMENT

The authors give thanks to David Meeker (dmeeker@ieee.org) for the use of the finite element CAD system *FEMM*. The authors also give thanks to the Brazilian Federal Agency for Postgraduate Studies (CAPES) for the sponsored access to several scientific web sites.

9. REFERENCES

[1] J.G.B. Wolff, H.D. Farias, A. Ramos, A.F.L. Nogueira, "Analysis and imaging in magnetic induction tomography using the impedance method", *Journal of Physics: Conference Series* **407** 012022 (2012) Available: http://dx.doi.org/10.1088/1742-6596/407/1/012022.

[2] E. Colin Cherry, "The duality between interlinked electric and magnetic circuits and the formation of transformer equivalent circuits", *Proc. Physical Society*, vol. 62B, pp. 101-111, 1949.

[3] C. Álvarez-Mariño, F. de Leon, X. M. López-Fernández, "Equivalent circuit for the leakage inductance of multiwinding transformers: unification of terminal and duality models", *IEEE Trans. on Power Delivery*, vol. 27, no. 1, 2012.

[4] N. Chiesa, Power transformer modelling advanced core model, MSc thesis, Politecnico di Milano, Italy, 2005, pp. 29-39.

[5] A.F.L. Nogueira, L.J.A.S. Maldonado, "Analysis of AC contactors combining electric circuits, time-harmonic finite element simulations and experimental work", *Journal of Research and Reviews in Applied Sciences*, vol. 14, no. 3, February 2013.

[6] D. Meeker, *Finite element method magnetics, user's manual*. Available: http://www.femm.info/Archives/doc/manual42.pdf

[7] A. Van der Bossche, V. Valchev, T. Filchev, "Improved approximation for fringing permeances in gapped inductors", in 37th Industry Applications Conference, IAS 2002, vol. 2, pp. 932-938.

[8] B. Forghani, E.M. Freeman, D.A. Lowther, P.P. Silvester, "Interactive modelling of magnetisation curves", *IEEE Trans. on Magnetics*, **MAG-18**, pp. 1070-1072, 1982.

[9] D.A. Lowther and P.P. Silvester, *Computer-aided design in magnetics*, Springer-Verlag, New York, 1986, pp. 13.

[10] L. Dixon, "Deriving the equivalent electrical circuit from the magnetic device physical properties", Magnetics Design Handbook (Ed. Texas Instruments Incorporated, USA, 2001).